Electronic supplementary information (ESI):

Self-supported nanoporous PtGa film as efficient multifunctional electrocatalyst for energy conversion

Ying Wang,[a] Zhenbin Wang,[a] Jie Zhang,[a] Chi Zhang,[b] Hui Gao,[a] Jiazheng Niu,[a] Zhonghua Zhang[a,b,*]

[a]Key Laboratory for Liquid-Solid Structural Evolution and Processing of Materials (Ministry of Education), School of Materials Science and Engineering, Shandong University, Jingshi Road 17923, Jinan 250061, P.R. China

[b]School of Applied Physics and Materials, Wuyi University, 22 Dongcheng Village, Jiangmen 529020, P.R. China

*Corresponding author. Email: zh_zhang@sdu.edu.cn (Z. Zhang)

Specific surface area calculation.

The mass of the np-PtGa foil was first weighed recording as m_1, and then the surface np-PtGa film was polished recording the mass of as-polished foils as m_2. The difference between m_1 and m_2 is the mass of the surface PtGa film. Three np-PtGa foil samples were prepared and treated as mentioned above, the corresponding surface PtGa films were measured to be 0.9, 0.9, and 1.0 mg, respectively. The mean value 0.93 mg was chosen as the mass of surface PtGa film, and then the mass of Pt (0.85 mg) in np-PtGa film could be obtained according to the EDX result. The electrochemically active area (EAA) was normalized to the mass of Pt to get the specific surface area.

Equation S1:

$$\mathbf{j_p=(2.99\times10^5)n(an_a)^{1/2}AC_0^*D_0^{1/2}v^{1/2}}$$

For a diffusion-controlled total irreversible electrooxidation reaction, the forward peak current (j_p) and the square root of scan rates ($v_{1/2}$) follows the above Equation, where n represents the total number of electrons involved in the reactions; a represents the electron transfer coefficient for the rate-determining step; n_a represents the electron transfer number in the rate-determining step; A represents the surface area of the electrode, which is a constant; C_0* represents the initial bulk concentration of the reactant; D_0 represents the diffusion coefficient. Because $C_0^*$and D_0 are the same in the same reaction solution, the slope of j_p versus $v^{1/2}$ is determined by $n(an_a)^{1/2}$. And $n(an_a)^{1/2}$ is related to the electron transfer involved in the electrooxidation, hence the higher slope value indicates the improved electrooxidation kinetics (enhanced electron transfer kinetics).[1]

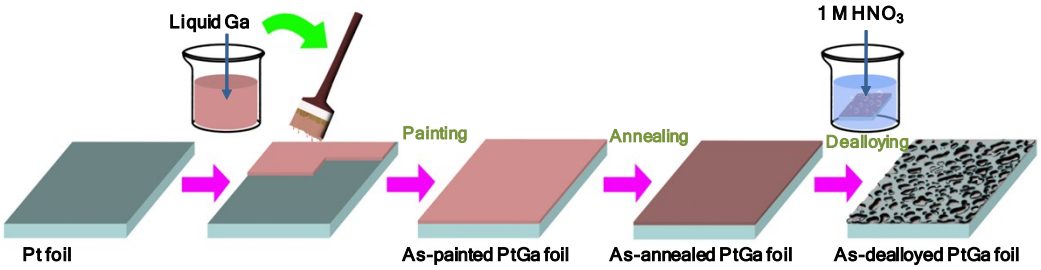

Figure S1. Schematic illustration showing the fabrication process of np-PtGa foil.

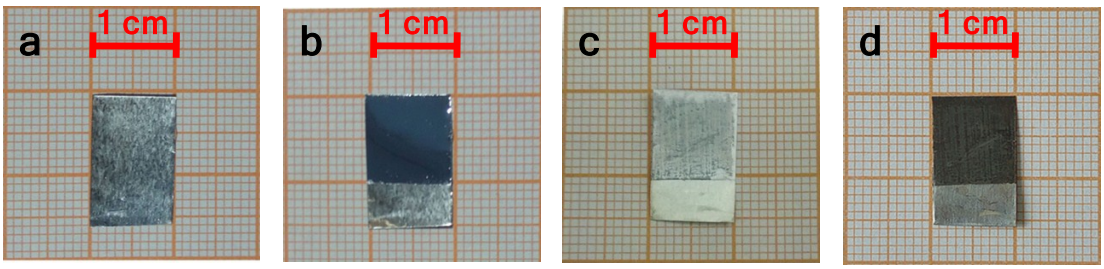

Figure S2. Photographs of (a) the pristine Pt foil, (b) the Pt foil covered with liquid Ga, (c) the annealed Pt foil covered with the Ga_2Pt phase, and (d) the as-dealloyed np-PtGa film (area: 1 × 1 cm^2) supported on the Pt foil.

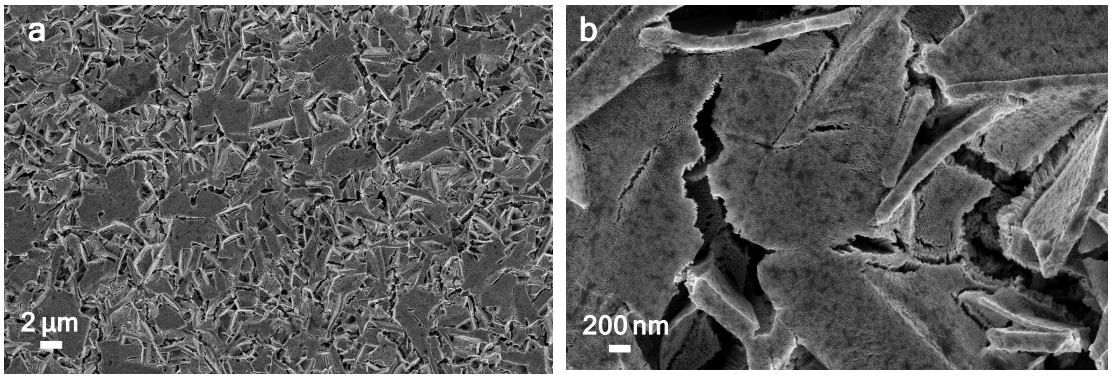

Figure S3. SEM images of the np-PtGa film supported on the Pt foil.

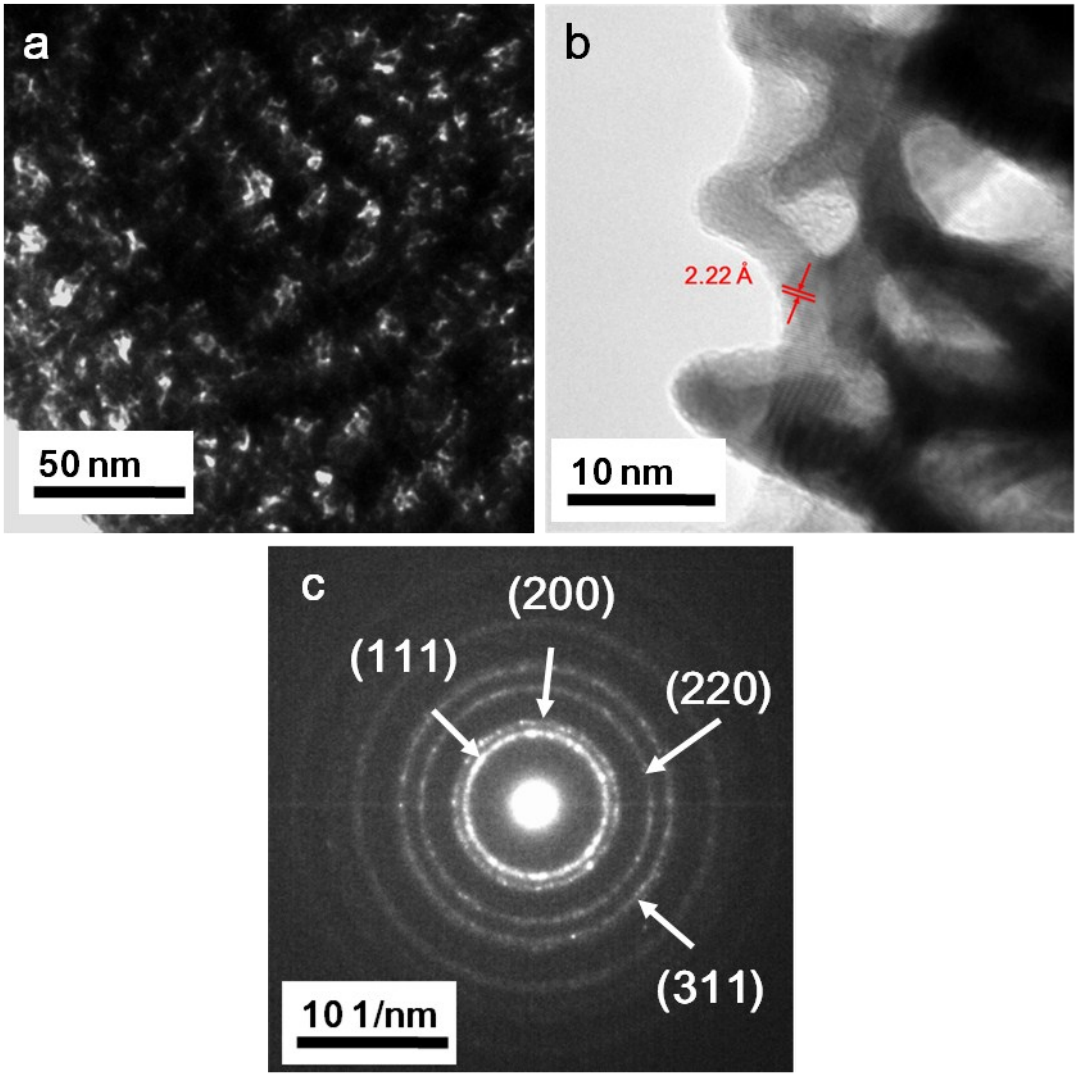

Figure S4. (a) TEM and (d) HRTEM images showing the microstructure of the np-PtGa film. (c) SAED pattern corresponding to (a).

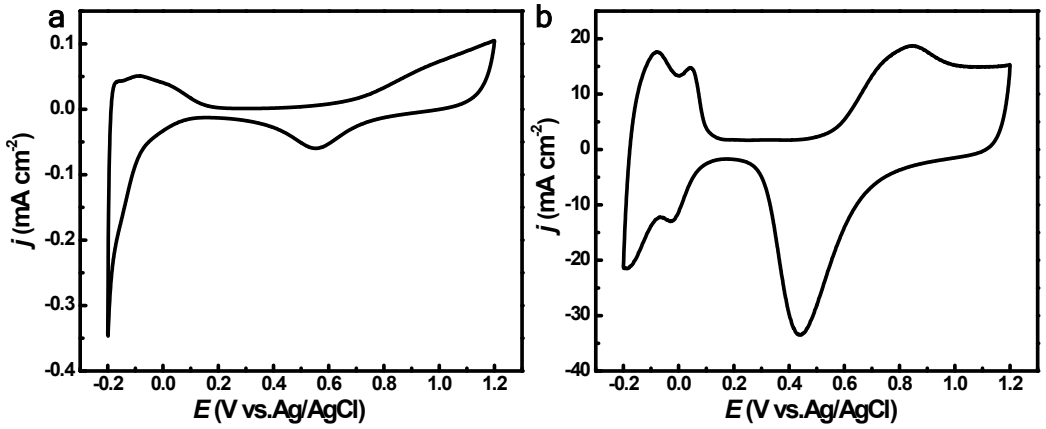

Figure S5. CVs of the (a) Pt foil and (b) np-PtGa foil in the N_2-purged 0.5 M H_2SO_4 solution. (Scan rate: 50 mV s^{-1})

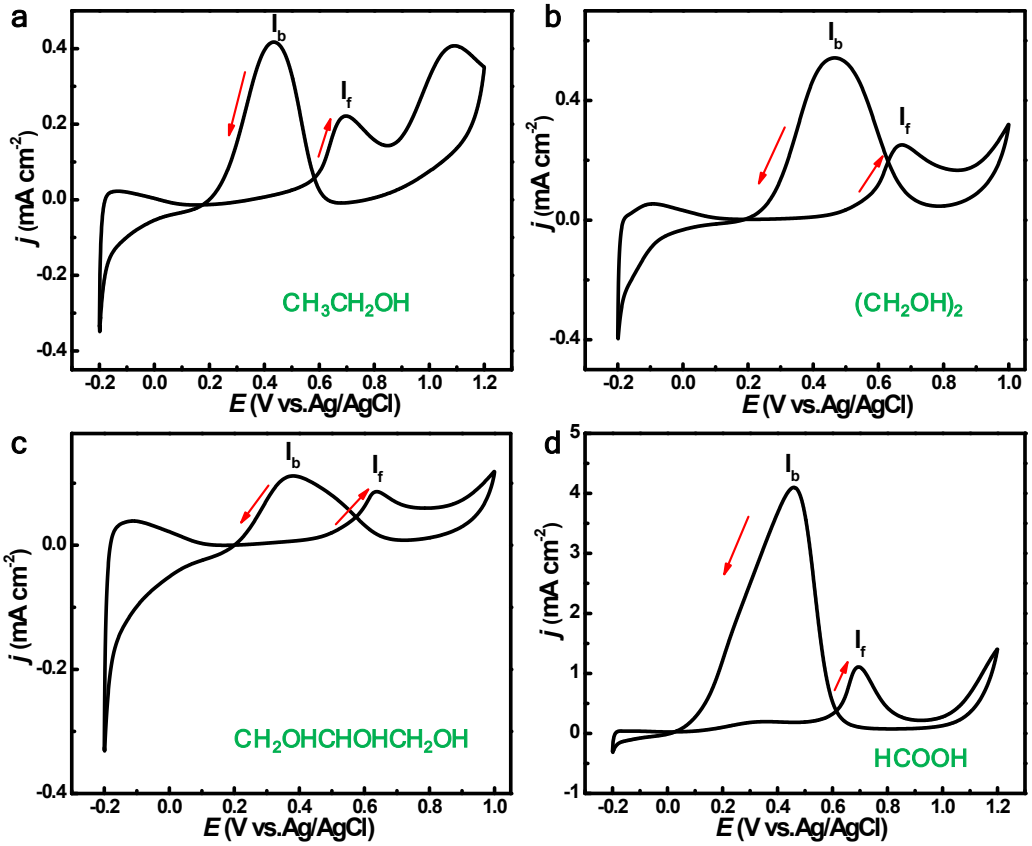

Figure S6. CVs of Pt foil in (a) 0.5 M H_2SO_4 + 0.5 M ethanol, (b) 0.5 M H_2SO_4 + 0.5 M EG, (c) 0.5 M H_2SO_4+0.5 M GLY and (d) 0.5 M H_2SO_4+0.5 M formic acid solutions at the scan rate of 50 mV s^{-1}.

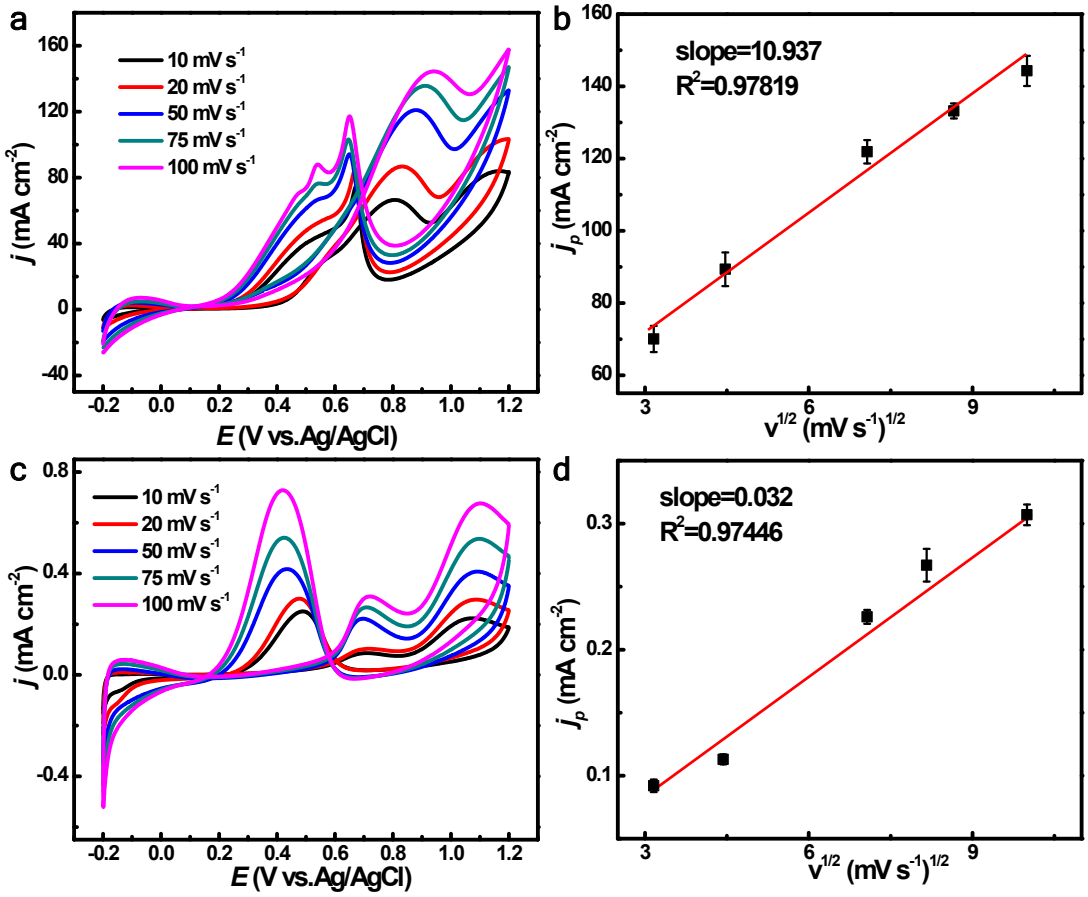

Figure S7. (a) CVs of the ethanol electrooxidation on np-PtGa foil in the 0.5 M H_2SO_4 +0.5 M ethanol solution at different scan rates and (b) the corresponding plot of j_p versus $v^{1/2}$. (c) CVs of the ethanol electrooxidation on Pt foil in the 0.5 M H_2SO_4 +0.5 M ethanol solution at different scan rates and (b) the corresponding plot of j_p versus the $v^{1/2}$.

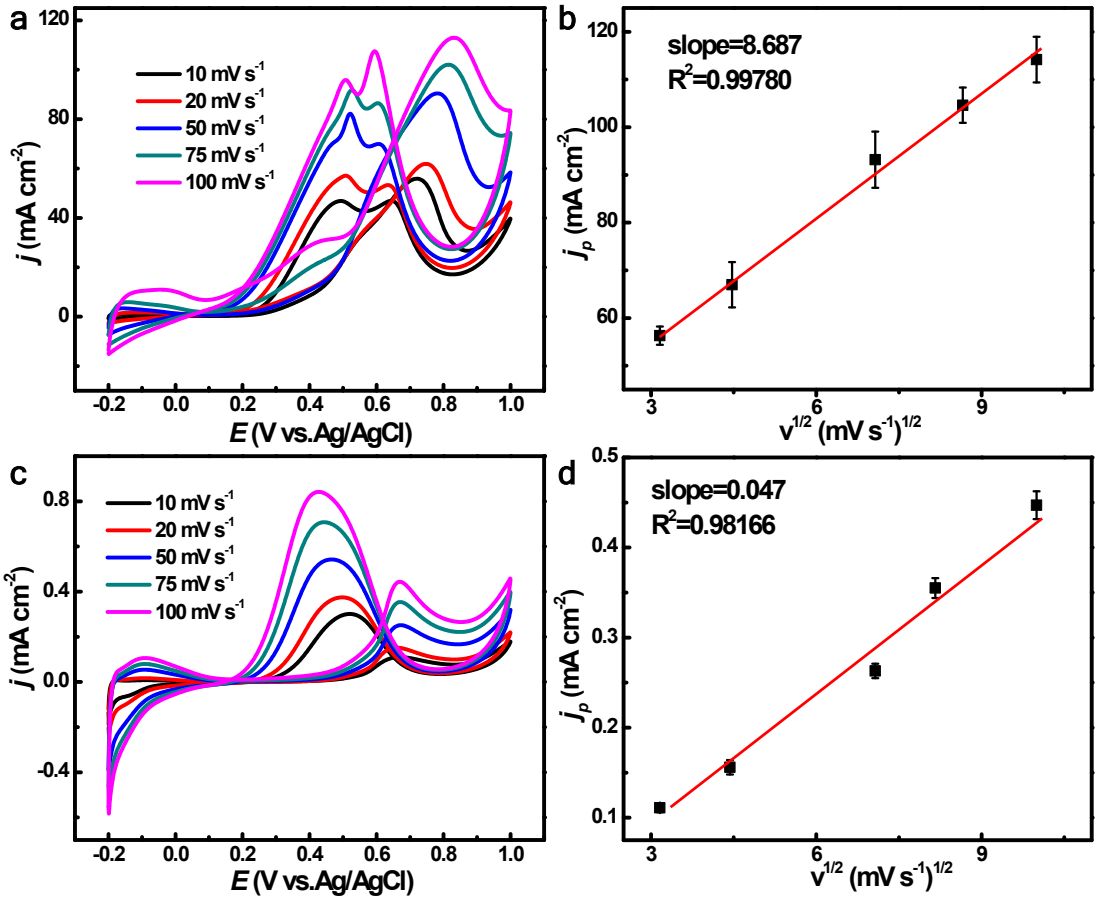

Figure S8. (a) CVs of the EG electrooxidation on np-PtGa foil in the 0.5 M H_2SO_4 +0.5 M EG solution at different scan rates and (b) the corresponding plot of j_p versus $v^{1/2}$. (c) CVs of the EG electrooxidation on Pt foil in the 0.5 M H_2SO_4 +0.5 M EG solution at different scan rates and (b) the corresponding plot of j_p versus the $v^{1/2}$.

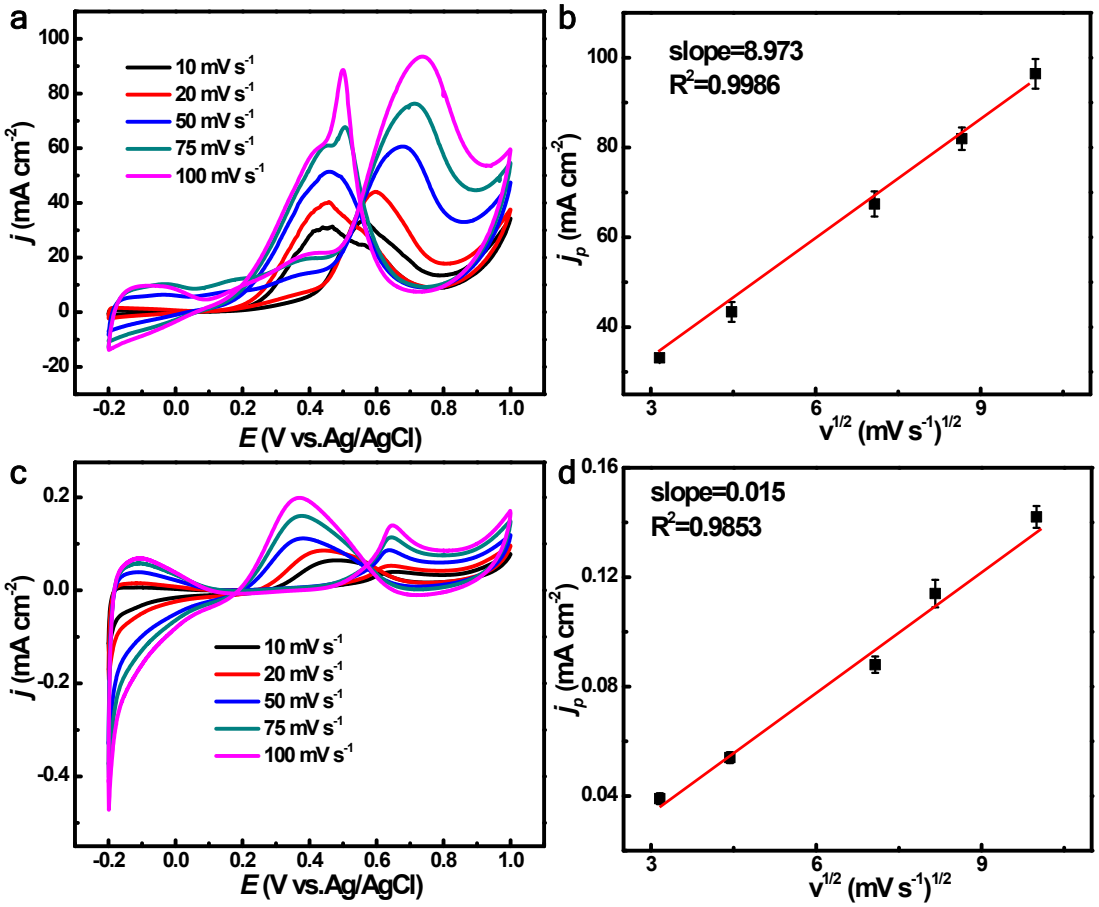

Figure S9. (a) CVs of the GLY electrooxidation on np-PtGa foil in the 0.5 M H_2SO_4 +0.5 M GLY solution at different scan rates and (b) the corresponding plot of j_p versus $v^{1/2}$. (c) CVs of the GLY electrooxidation on Pt foil in the 0.5 M H_2SO_4 +0.5 M GLY solution at different scan rates and (b) the corresponding plot of j_p versus the $v^{1/2}$.

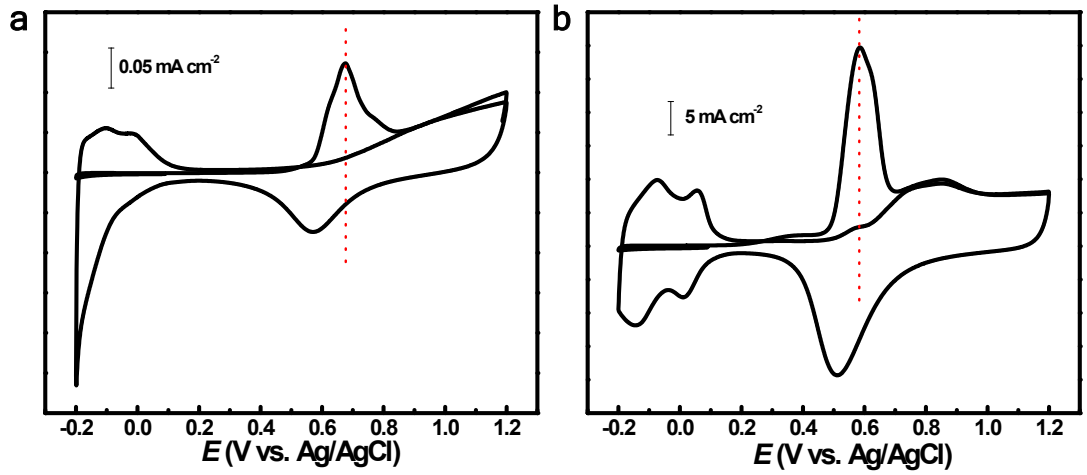

Figure S10. Electrochemical CO-stripping curves of (a) Pt foil and (b) np-PtGa foil in the 0.5 M H_2SO_4 solution.

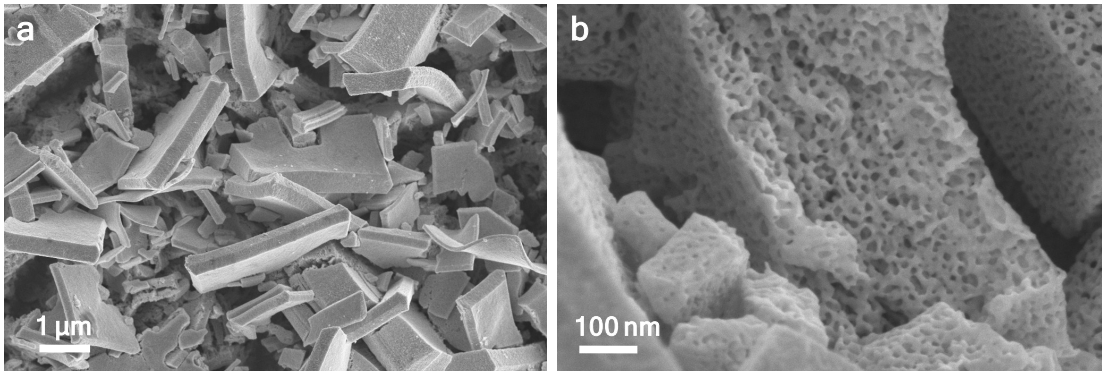

Figure S11. SEM images showing the morphology of np-PtGa film after the potential cycles.

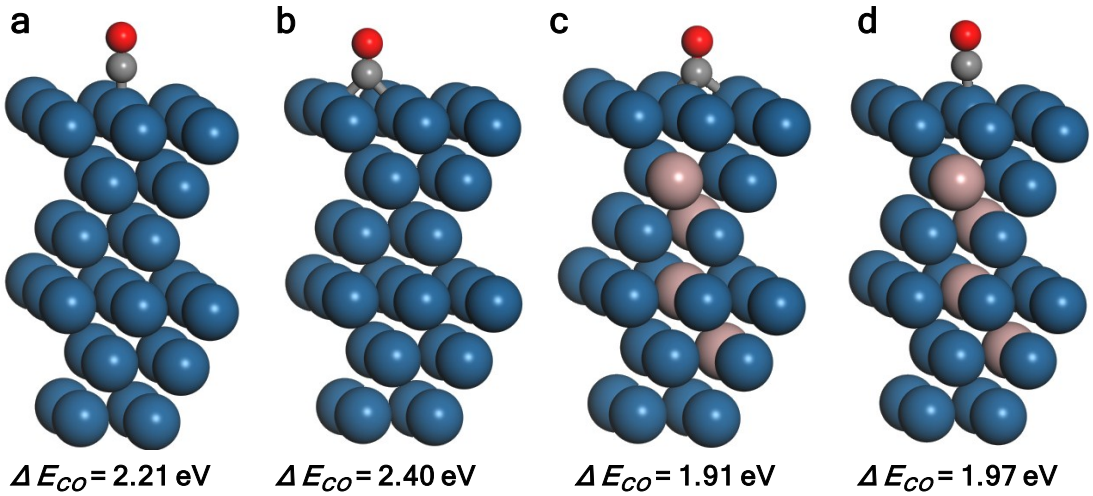

Figure S12. The schematic model of CO adsorbed on (a) the top site of Pt (111), (b) the brige site of Pt (111), (c) the f.c.c site of PtGa (111), and (d) the top site of PtGa (111).

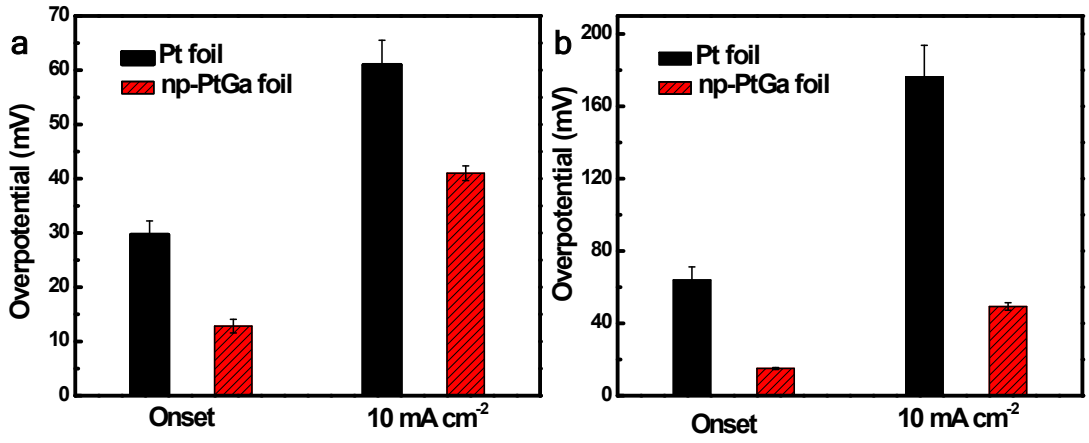

Figure S13. The onset potentials and overpotentials at 10 mA cm^{-2} for np-PtGa foil and Pt foil in (a) 0.5 M H_2SO_4 and (b) 1.0 M KOH.

Table S1. Comparison of the HER performance for our np-PtGa foil with that of previously reported state-of-the-art noble metal-based HER electrocatalysts in alkaline solutions.

catalysts	*ref*	Overpotential (mV@ mA cm^{-2})	Tafel slope (mV dec^{-1})	electrolytes
Our np-PtGa foil	This work	**50@10**	**55**	1.0 M KOH
Pd@PtCu nanocrystal	2	60@10	--	0.1 M KOH
Hcp PtNi nano-multipods	3	65@10	78	0.1 M KOH
PdPt heterostructure	4	71@10	31	1.0 M KOH
Mesoporous Fe–	5	74@10	--	1.0 M KOH

Pt Smooth Thin Fil

ms

Mesporous FePt film				
PtNi nanocages	6	104@10	73	0.1 M KOH
Pt-NiFe LDH	7	101@10	127	1.0 M KOH
Pd Nanonetwork	8	110@10	121	1.0 M KOH
PdNi/CNFs	9	187@10	93	1.0 M KOH
PdTe NMs/rGO	10	97@10	--	1.0 M KOH
Au-Ru Nanowires	11	50@10	30.8	1.0 M KOH
$Ni@Ni(OH)_2/Pd/rGO$	12	76@10	70	1.0 M KOH
$Pd-Mn_3O_4$	13	115@10	--	0.5 M KOH
$Au-Co(OH)_2$	14	424	54	0.1 M KOH
Pt NWs/SL-Ni(OH)	15	57.8@4	--	0.1 M KOH
		85.5@4		1.0 M KOH
Pt_3Ni frames/$Ni(OH)_2$/C	16	~59@4	--	0.1 M KOH
$Ni(OH)_2$ modified Pt surface	17	~95@4	--	0.1 M KOH

References

1 W. Hong, C. Shang, J. Wang, and E. Kang, *Energy Environ. Sci.,*, 2018, **3**, 940-945.

2 M. Bao, I. S. Amiinu, T. Peng, W. Li, S. Liu, Z. Wang, Z. Pu, D. He, Y.

Xiong and S. Mu, *ACS Energy Lett.*, 2018, **3**, 940-945.

3 Z. Cao, Q. Chen, J. Zhang, H. Li, Y. Jiang, S. Shen, G. Fu, B. A. Lu, Z. Xie and L. Zheng, *Nat. Commun.*, 2017, **8**, 15131-15137.

4 J. Fan, K. Qi, L. Zhang, H. Zhang, S. Yu and X. Cui, *ACS Appl. Mater. Interfaces*, 2017, **9**, 18008-18014.

5 E. Isarain-Chavez, M. D. Baro, C. Alcantara, S. Pane, J. Sort and E. Pellicer, *ChemSusChem*, 2018, **11**, 367-375.

6 Z. Cao, H. Li, C. Zhan, J. Zhang, W. Wang, B. Xu, F. Lu, Y. Jiang, Z. Xie and L. Zheng, *Nanoscale*, 2018, **10**, 5072-5077.

7 S. Anantharaj, K. Karthick, M. Venkatesh, T. V. S. V. Simha, A. S. Salunke, L. Ma, H. Liang and S. Kundu, *Nano Energy*, 2017, **39**, 30-43.

8 H. Begum, M. S. Ahmed and S. Jeon, *ACS Appl. Mater. Interfaces*, 2017, **9**, 39303-39311.

9 J. Chen, J. Chen, D. Yu, M. Zhang, H. Zhu and M. Du, *Electrochim. Acta*, 2017, **246**, 17-26.

10 L. Jiao, F. Li, X. Li, R. Ren, J. Li, X. Zhou, J. Jin and R. Li, *Nanoscale*, 2015, **7**, 18441-18445.

11 Q. Lu, A.-L. Wang, Y. Gong, W. Hao, H. Cheng, J. Chen, B. Li, N. Yang, W. Niu, J. Wang, Y. Yu, X. Zhang, Y. Chen, Z. Fan, X.-J. Wu, J. Chen, J. Luo, S. Li, L. Gu and H. Zhang, *Nat. Chem.*, 2018, **10**, 456-461.

12 Z. Deng, J. Wang, Y. Nie and Z. Wei, *J. Power Sources*, 2017, **352**, 26-33.

13 C. Ray, S. Dutta, Y. Negishi and T. Pal, *Chem. Commun.*, 2016, **52**, 6095-

6098.

14 B. Sidhureddy, A. R. Thiruppathi and A. Chen, *J. Electroanal. Chem.*, 2017, **794**, 28-35.

15 H. Yin, S. Zhao, K. Zhao, A. Muqsit, H. Tang, L. Chang, H. Zhao, Y. Gao and Z. Tang, *Nat. Commun.*, 2015, **6**, 6430-6437.

16 C. Chen, Y.Kang, Z. Huo, Z. Zhu, W. Huang, H.L. Xin, J.D. Snyder, D. Li, P. Yang, V.R. Stamenkovic, *Science*, 2014, **343**, 1339-1443..

17 N. Danilovic, R. Subbaraman, D. Strmcnik, K. C. Chang, A. P. Paulikas, V. R. Stamenkovic and N. M. Markovic, *Angew. Chem. Int. Ed.*, 2012, **51**, 12495-12498.